Saturated Adaptive Control of Muscle-like Compliant Manipulation Systems

Konrad Siedler*, Joachim Steigenberger** and Carsten Behn*
*Department of Mechanical Engineering, Technical Mechanics Group, Technische Universität Ilmenau, Ilmenau, Germany
**Institute of Mathematics, Technische Universität Ilmenau, Ilmenau, Germany

Summary. In this paper, actuators with muscle-like properties are considered to control a compliant manipulation system. The work examines the question under what conditions an intensity control for antagonistic muscle pairs is possible. Because of the natural paragon muscle, we have to consider limited control strategies using muscle intensities. The goal is to clarify how different approaches for the intensity can be implemented using several strengths of actuators or differing feedback control strategies. Therefore, numerical simulations of the robotic structure with two degrees of freedom are performed. As a result, this work shows up that a saturated adaptive tracking control strategy is most suited for muscles of different strengths.

Introduction

To actuate and/or to control (compliant) structures in a new and alternate way, muscle-like actuators are increasingly used. A typical example to demonstrate the effectiveness of developed control schemes is the choice of a (inverted) pendulum with DoF ≥ 2, see [1] and [4]. The double pendulum system chosen here is inspired by a biological example: human arm. This structure consists of an upper arm and a forearm with antagonistically arranged muscle pairs, which describes a plane movement.
The double pendulum robot arm is of a simplified SCARA type (selective compliance assembly robot arm). Figure 1 shows the functional principle and the mechanical quantities of the system.

m_i	mass of element
J_i	mass moment of inertia w.r.t. to s_i
s_i	center of mass m_i
l_i	distances between joints
r_i	distances between center of masses
ϑ_i	(relative) angle of pivot joint
$C_{C\,k}$	contractile muscle-like element

for i = 1,2
k = 1 ... 4

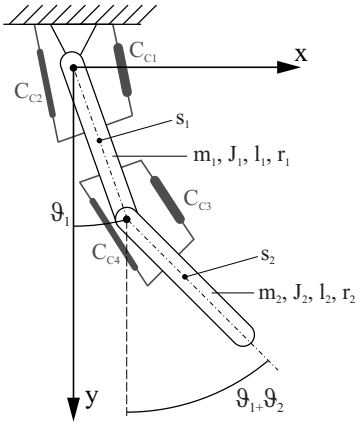

Figure 1: Underlying double pendulum structure (black) with actuator arrangement (grey).

To determine the equations of motion using Euler-Lagrange equations of the 2nd kind, the generalized coordinates $q_1 := \vartheta_1$ and $q_2 := \vartheta_2$ are chosen. The resulting equations are represented in the following matrix-vector notation [2]:

$$M(q)\ddot{q} + C(q,\dot{q})\dot{q} + G(q) = u, \tag{1}$$

$$\text{with: } M(q) = \begin{pmatrix} m_1\, r_1^2 + J_1 + m_2\left[l_1^2 + r_2^2 + 2\, l_1\, r_2 \cos(q_2)\right] + J_2 & m_2\left[r_2^2 + l_1\, r_2 \cos(q_2)\right] + J_2 \\ m_2\left[r_2^2 + l_1\, r_2 \cos(q_2)\right] + J_2 & m_2\, r_2^2 + J_2 \end{pmatrix},$$
$$C(q,\dot{q})\,\dot{q} = \begin{pmatrix} -m_2\, l_1\, r_2 \sin(q_2)\left[\dot{q}_2^2 + 2\dot{q}_1\,\dot{q}_2\right] \\ \dot{q}_1^2\, m_2\, l_1\, r_2 \sin(q_2) \end{pmatrix},\ G(q) = \begin{pmatrix} \sin(q_1)[m_1\, g\, r_1 + m_2\, g\, l_1] + m_2\, g\, r_2 \sin(q_1+q_2) \\ m_2\, g\, r_2 \sin(q_1+q_2) \end{pmatrix} \tag{2}$$

Control strategies

In order to control such system using muscle-like actuators and their intensities, we have to guarantee that the control variable u is bounded a-priori. For this, a saturated feedback strategy is used in [6] which is based on [7], allowing for restricted control inputs. To get a good stabilization result, the user has to choose some tuning factors. But, controlling dynamical systems normally requires detailed knowledge of the system at hand, which can be both very difficult and time consuming to obtain as the system complexity increases. Hence, the tuning is often done by a trial&error-method, which is unsatisfactory.
Therefore, another and significantly faster solution can be achieved using an adaptive control strategy according to [8]. In the following, different controllers are presented under which the best results are sought, whereby the index i points out

the belonging of the controllers to the joints $i = 1, 2$.
For adaptive ways to generate the control variable $u_i(t)$ there is chosen a PID-feedback structure:

$$u_i(t) = -k_i(t)\, e_i(t) - \kappa_i\, k_i(t)\, \dot{e}_i(t) - \eta_i\, k_i(t) \int_0^t e_i(\tau)\, d\tau \tag{3}$$

One way to design the adaptive gain factor is the one according to the λ-stabilizing controller, [5]:

$$\dot{k}_i(t) = \gamma_i \begin{cases} (\|e_i(t)\| - \lambda_i)^2\,, & \text{for } \|e_i(t)\| \geq \lambda_i \\ 0\,, & \text{for } \|e_i(t)\| < \lambda_i \end{cases} \tag{4}$$

Additionally, there is an advanced type of λ-stabilization of [2] with further prominent features, presented in [8]:

$$\dot{k}_i(t) \quad = \gamma_i \left\{ \begin{array}{ccc} (|e_i(t)| - \varepsilon_i\lambda_i)^2 & \text{for} & \varepsilon_i\lambda_i + 1 \leq |e_i(t)| \\ (|e_i(t)| - \varepsilon_i\lambda_i)^{\frac{1}{2}} & \text{for} & \varepsilon_i\lambda_i \leq |e_i(t)| < \varepsilon_i\lambda_i + 1 \\ 0 & \text{for} & |e_i(t)| < \varepsilon_i\lambda_i \,\wedge\, t - t_{ei} < t_{di} \\ -\delta_i(|e_i(t)|, \varepsilon_i\lambda_i)\, k_i(t) & \text{for} & |e_i(t)| < \varepsilon_i\lambda_i \,\wedge\, t - t_{ei} \geq t_{di} \\ \multicolumn{3}{c}{\text{with } \delta_i(|e_i(t)|, \varepsilon_i\lambda_i) := \sigma_i \cdot \left(1 - \dfrac{|e_i(t)|}{\varepsilon_i\lambda_i}\right)} \end{array} \right\} \tag{5}$$

Beside other new abilities with this adaptation law, the gain factor has the possibility to decrease its value according to the exponential decay after entering the λ-tolerance area. This safeguards the gain factor against to high feedback values.

Remind, the system consists of four muscles C_{Cj}, $j = 1, \ldots, 4$, controlled by the input variables u_1 and u_2. Their levels are merged by an intensity controlling. Because of the antagonistic arrangement of the muscles, it is possible to convert the control variables u_i into intensities w_j, $j = 1, \ldots, 4$, using the muscle characteristic curve of HILL (force-velocity-relation) [9]. An approximation of this relation uses the $\arctan(\cdot)$ which results in the following analytical presentation [2]:

$$F(t) = w(t)\, h(\dot{q}(t)), \quad \text{with} \quad h(\cdot) = a_j^* - b_j^* \arctan(\cdot), \quad a_j^*, b_j^* \in \mathbb{R}^+, j = 1, \ldots, 4 \tag{6}$$

here $F(t)$ - muscle force, $w(t)$ - intensity, $h(\dot{q}(t))$ - function of the characteristic muscle curve.
Because of the mechanical behavior of the joints, an angular change of $\dot{q}_1 > 0$ represents a contraction of the muscle C_{C1} and an extension of C_{C2}. This leads to the relation of the control u_1 and intensities w_1 and w_2 (analogous u_2):

$$u_1 = h_1(\dot{q}_1)w_1 - h_2(-\dot{q}_1)w_2 \quad \text{and} \quad u_2 = h_3(\dot{q}_2)w_3 - h_4(-\dot{q}_2)w_4 \tag{7}$$

using the complimentary-slackness conditions

$$w_1\, w_2 = 0\,, \quad w_3\, w_4 = 0\,. \tag{8}$$

In order to ensure that the maximum muscle performance will not exceed, the control variable has to be saturated. In doing this, the complete range of the characteristic muscle curve has to be used:

$$\begin{array}{l} -h_2(-\dot{q}_1)w_2 \geq u_1 \leq h_1(\dot{q}_1)w_1 \quad \text{with } w_1 = 1 \text{ for } u_1 > h_1(\dot{q}_1) \text{ and } w_2 = 1 \text{ for } u_1 < -h_2(-\dot{q}_1) \\ -h_4(-\dot{q}_2)w_4 \geq u_2 \leq h_3(\dot{q}_2)w_3 \quad \text{with } w_3 = 1 \text{ for } u_2 > h_3(\dot{q}_2) \text{ and } w_4 = 1 \text{ for } u_2 < -h_4(-\dot{q}_2) \end{array} \tag{9}$$

Remind the complimentary-slackness conditions (8): if $w_1 \neq 0$, $w_2 = 0$.
So, beyond the maximum performance, the value of the control variable is set to the finite (given) limit.

Another, more elegant way is to use a saturated controller strategy like shown in [7]. The saturated controller is limited due to its design structure in using a saturation function. Hence, an extra saturation using (9) is not necessary for this controller:

$$\left. \begin{array}{l} \dot{q}_{ci} = -k_{1i}\, q_{ci} - k_{2i}\, \text{sat}(q_{ci} - e_i) \\ u_{pi} = k_{2i}\, \text{sat}(q_{ci} - e_i) + \dfrac{\partial}{\partial q_{pi}} U_p(q_{pi}) \\ \text{with } U_p(q_p) = (-m_1 g r_1 - m_2 g l_1)\cos(q_{p1}) - m_2 g r_2 \cos(q_{p1} + q_{p2}) \\ \text{and} \quad \Delta\, q_{pi} = q_{pi} - q_{di} \end{array} \right\} \tag{10}$$

For the following simulations, the sat$(\cdot)$-function is replaced by the $\tanh(\cdot)$-function.

Simulations

The following parameters of system (2) are chosen arbitrarily [8]:

system parameters: $m_1 = m_2 = 2$, $r_1 = r_2 = 1$, $l_1 = l_2 = 2$, $J_1 = J_2 = 1$,

muscle parameters: $a_1^* = 110$, $a_2^* = 60$, $a_3^* = a_4^* = 25$, $b_j^* := \frac{2a_j^*}{\pi}$, with $j = 1, \ldots, 4$

The initial position is $(q_1(0), \dot{q_1}(0), q_2(0), \dot{q_2}(0)) = (0, 0, 0, 0)$, the targeted one $(q_1(0), \dot{q_1}(0), q_2(0), \dot{q_2}(0)) = (\pi, 0, 0, 0)$.

Simulation 1 - classical λ-stabilizer without saturation:
In this simulation, feedback law (3) *and adaptation law* (4) *to system* (1) *without an external saturation. For this first simulation, the following control parameters are chosen:* $\kappa_i = 0.2$, $\eta_i = 0.05$, $\lambda_i = 0.2$, $\gamma_i = 100$. *Then, Figures 2 and 3 show the results. The stabilization of the target position takes place very quickly, see Figure 2(left). However, it is clearly*

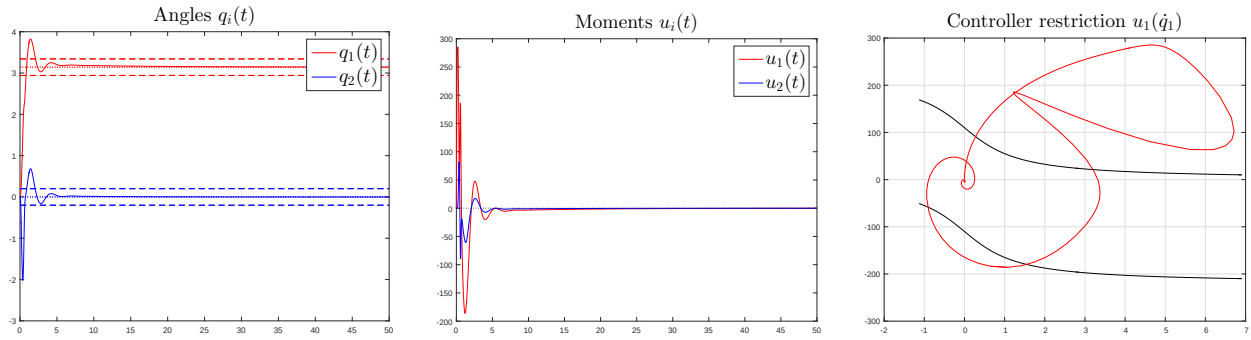

Figure 2: Joints angles q_i (left), control inputs u_i (middle), feasible range of u_1 (right).

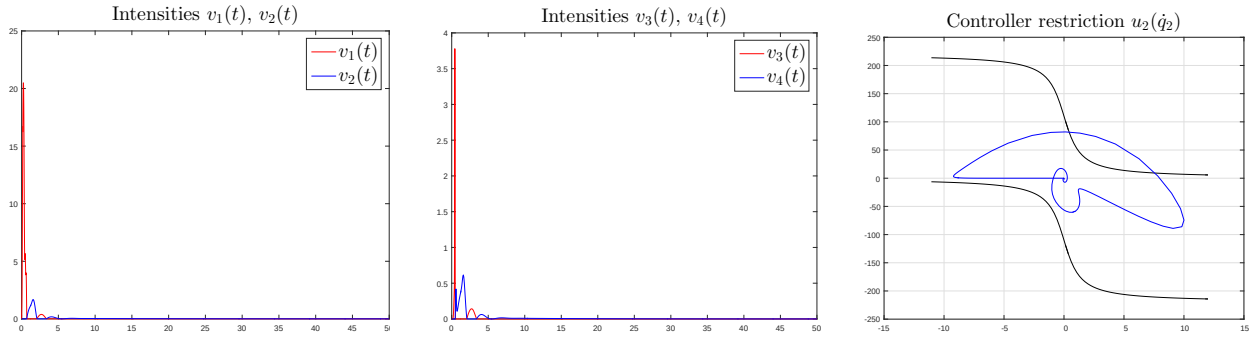

Figure 3: Intensities of the muscles C_{C1} and C_{C2} (left), intensities of the muscles C_{C3} and C_{C4} (middle), feasible range of u_2 (right).

to see, that the necessary muscle performance is more than 20 times larger as the maximum possible one, exemplarily shown in the feasible ranges (see Figs. 2 and 3(right)). To ensure feasibility, the muscle performance has to be saturated with the external rule of saturation (9).

Simulation 2 - classical λ-stabilizer with saturation:
Here, we apply feedback law (3) *and adaptation law* (4) *to system* (1)*, with a prescribed external saturation* (9). *For this simulation, we use same control parameter values as Simulation 1. The numerical results are presented in Figures 4 and 5.*

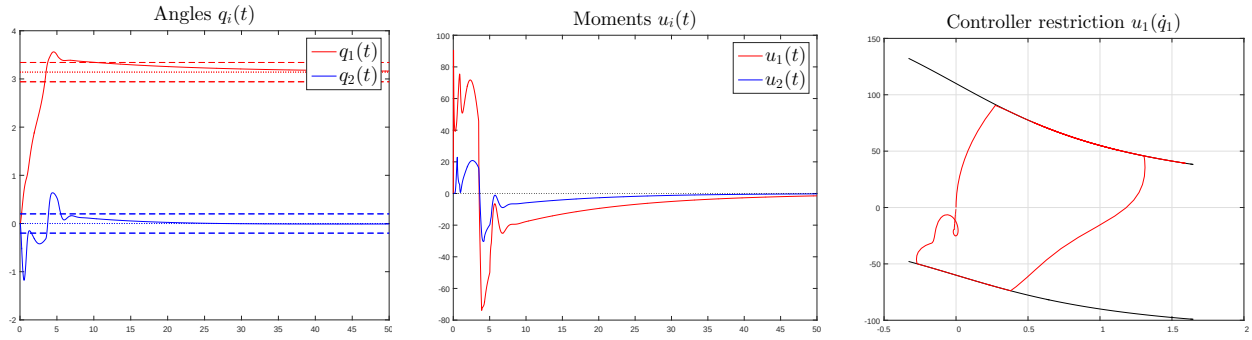

Figure 4: Joints angles q_i (left), control inputs u_i (middle), feasible range of u_1 (right).

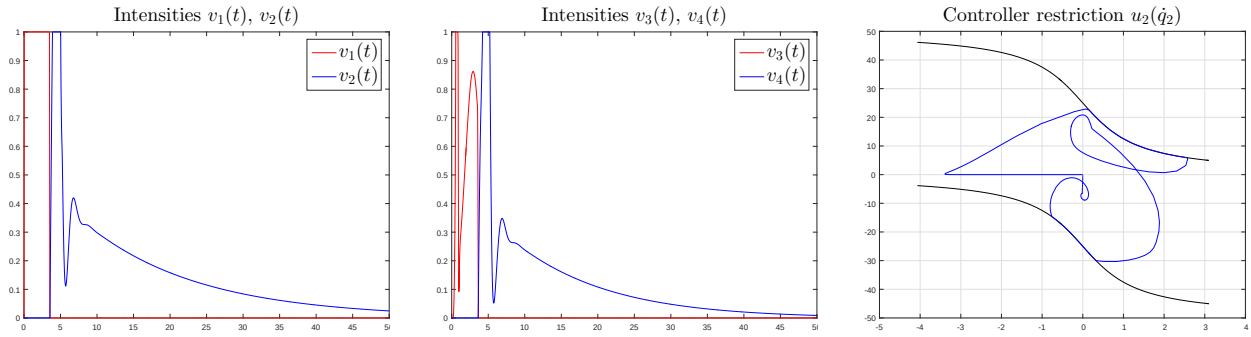

Figure 5: Intensities of the muscles C_{C1} and C_{C2} (left), intensities of the muscles C_{C3} and C_{C4} (middle), feasible range of u_2 (right).

With this external saturation, the system does not get the required/necessary control resources, so the overall movement has to be slowed down.
After entering the λ-tolerance area, the gain factors still stay constant at the values of about $k_1 \approx 848$ and $k_2 \approx 64$ due to the adaptation law (4)*. Thereby, it can be seen, that the necessary control value u_2 allows for choosing weaker muscles in joint* 2*. An exchange of suited muscles will result in a higher utilization of these muscles with respect to the intensities. Nevertheless, the presented control strategy is able to stabilize the system with muscles of different strengths.*

Simulation 3 - classical λ-stabilizer with new adaptation and saturation:
In comparison to the previous simulations, the system here is controlled with the adaption law (5)*, using $\kappa_i = 0.2$, $\eta_i = 0.05$, $\lambda_i = 0.2$, $\varepsilon_i = 0.7$, $\gamma_i = 100$, $\sigma_i = 0.1$, $t_{di} = 2$ from [8]. Figures 6 and 7 show the results.*

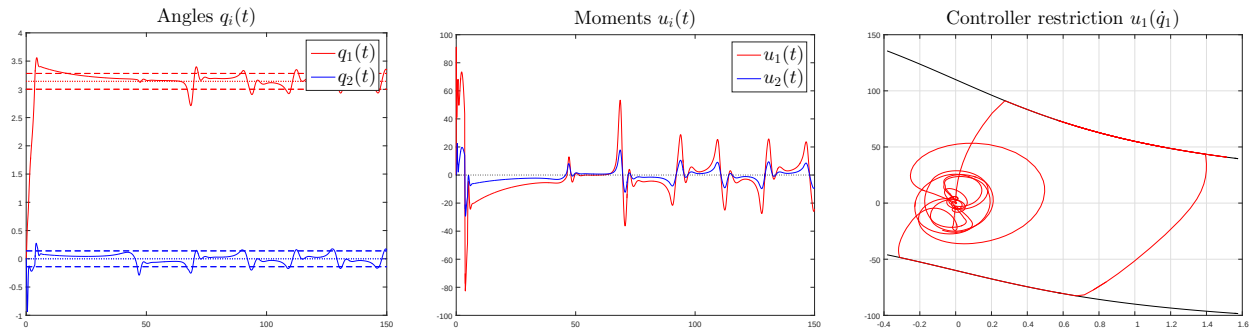

Figure 6: Joints angles q_i (left), control inputs u_i (middle), feasible range of u_1 (right).

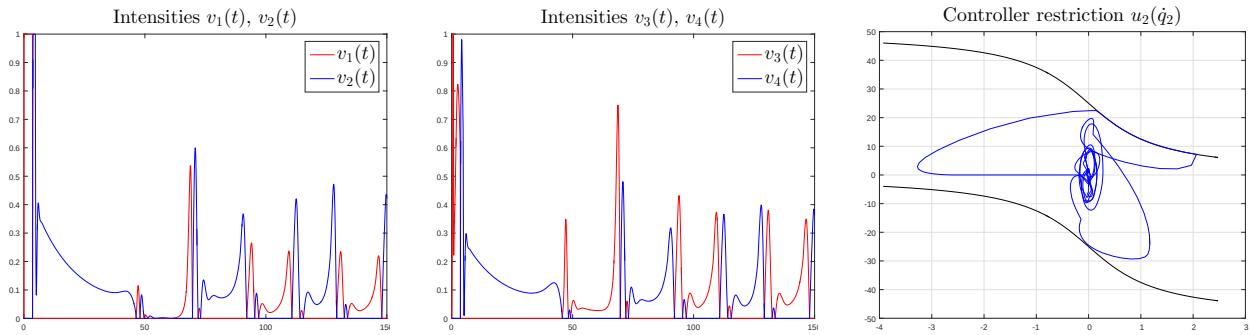

Figure 7: Intensities of the muscles C_{C1} and C_{C2} (left), intensities of the muscles C_{C3} and C_{C4} (middle), feasible range of u_2 (right).

Because of the chosen control parameters, at the beginning, the system performance is similar to the behavior in Simulation 1 and 2 using (4)*. At around $t > 30$ the influence of the new adaptation law on the system behavior can be seen in observing $q_2(t)$: The angle begins to sway, because of the decreasing gain factor. At $t = 46\,s$ the angle q_2 leaves the λ-tolerance area (and at about $t = 67\,s$ the angle q_1, too), so that the angle has to get re-stabilized. Figure 8 shows the behavior of the gain factor.*

Simulation 4 - saturated controller (10) / parameter set 1:
Only a very low number of system parameters have to be tuned for this controller (10)*: $k_{1i} = 1$, $k_{2i} = 1$, according to [6]. Then, Figures 9 and 10 show the results. For the simulations with this controller* (10)*, symmetric muscle parameters are chosen: $a_j^* = 110$, $b_j^* := \frac{2a_j^*}{\pi}$, with $j = 1, \ldots, 4$.*
Applying this new controller (10) *with its parameters to the system, the output/angles converges to the targeted position*

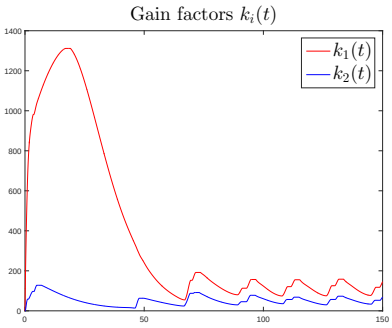

Figure 8: Behavior of the gain factor of simulation 2.

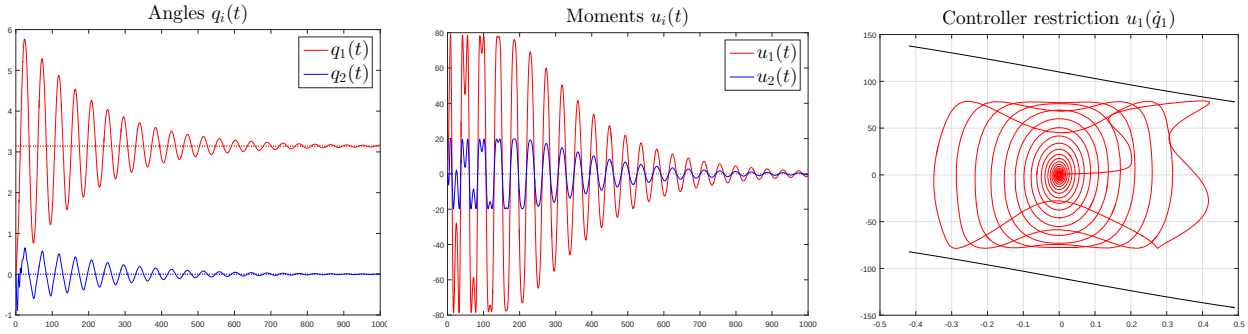

Figure 9: Joints angles q_i (left), control inputs u_i (middle), feasible range of u_1 (right).

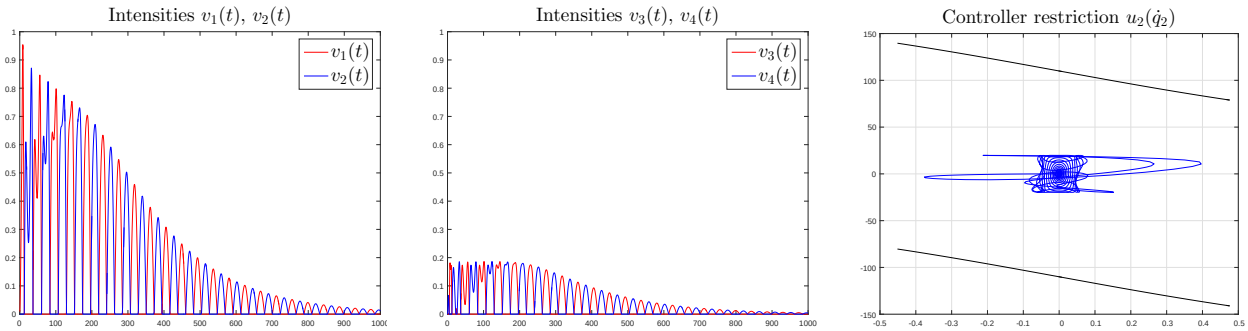

Figure 10: Intensities of the muscles C_{C1} and C_{C2} (left), intensities of the muscles C_{C3} and C_{C4} (middle), feasible range of u_2 (right).

very slowly. The overshooting and oscillation follows from the arbitrary choice of the factors k_{1i}, which seems unfavorable.

The following Simulation 5 shall present improved results in choosing appropriate parameters.

Simulation 5 - saturated controller (10) / parameter set 2:
Again, we apply (10) *to the system. Here, we try to reduce/improve the unlike behavior of the system in Figures 9 and 10 in choosing the following control parameters k_{1i}: $k_{1i} = 0$, $k_{2i} = 1$. The resulting behavior is numerically determined, see Figures 11 and 12.*

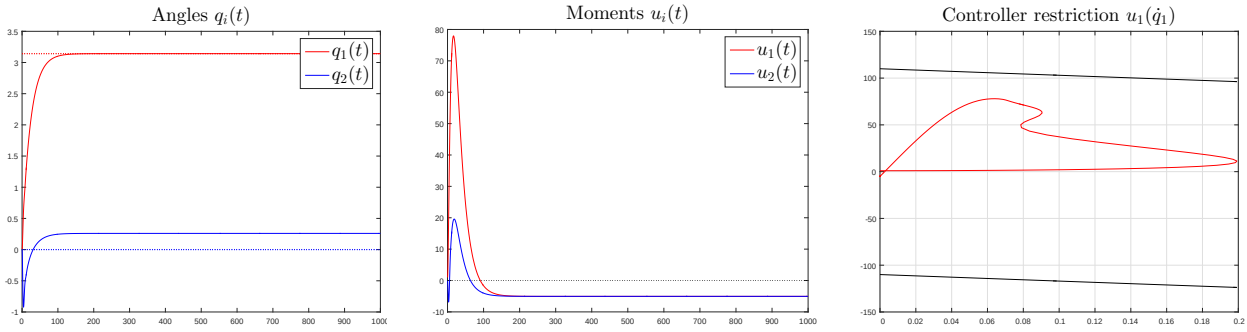

Figure 11: Joints angles q_i (left), control inputs u_i (middle), feasible range of u_1 (right).

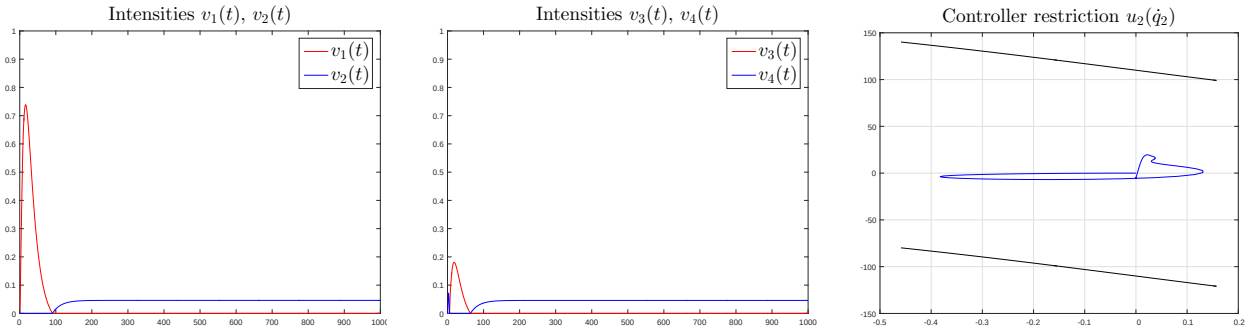

Figure 12: Intensities of the muscles C_{C1} and C_{C2} (left), intensities of the muscles C_{C3} and C_{C4} (middle), feasible range of u_2 (right).

In zeroing the parameters k_{1i}, the overshoot of the angles can be eliminated, only especially angle q_2 exhibits a constant error. With values about $k_{1i} \approx 0.01$, this error can be diminished, but with a relative high overshoot in matters of the low values.
Summarizing, a stabilization result can be achieved, but to the expense of a very slow convergence. Even with values $k_{1i} > 0$ the velocity of the controller is not significantly rising, it behaves in opposite way: The higher these factors are, the stronger the overshooting gets, so that the angles are oscillating up to more than $1000\,s$ before stabilizing the position.

Because of the simulation results in Simulation 4 and 5, we do not focus further on controller (10) and present some improved system behaviors in tuning some parameters in the following, according to [3].

Simulation 6 - advanced λ-stabilizer with new adaptation and saturation:
All applied adaptation laws until now exhibit the fact, that every gain parameter is only based on one error variable (difference between angle and desired one). Better results can be achieved in incorporating both error variables to every gain adaptation law. That means, we set up an error vector $e(t) = \left(e_1(t) e_2(t)\right)^T$ and use it for the adaptation applying the maximum-norm $||e(t)||_\infty$. The simulation results are given in Figures 13 and 14, using the same control parameters as in Simulation 3.

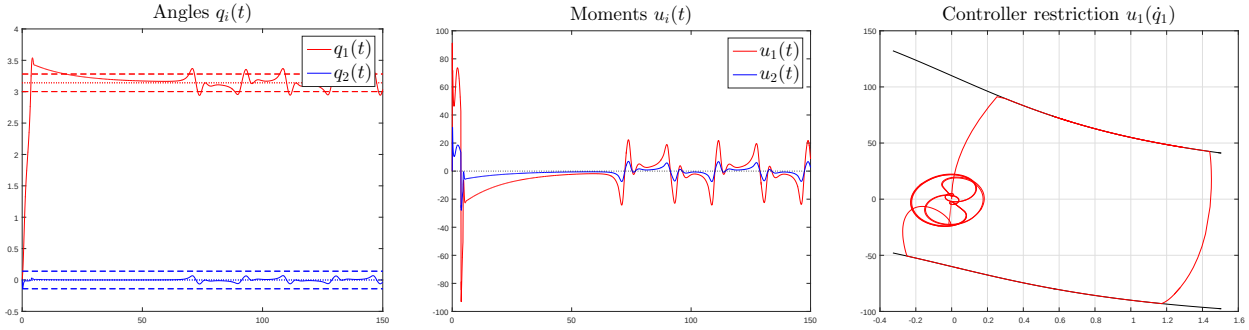

Figure 13: Joints angles q_i (left), control inputs u_i (middle), feasible range of u_1 (right).

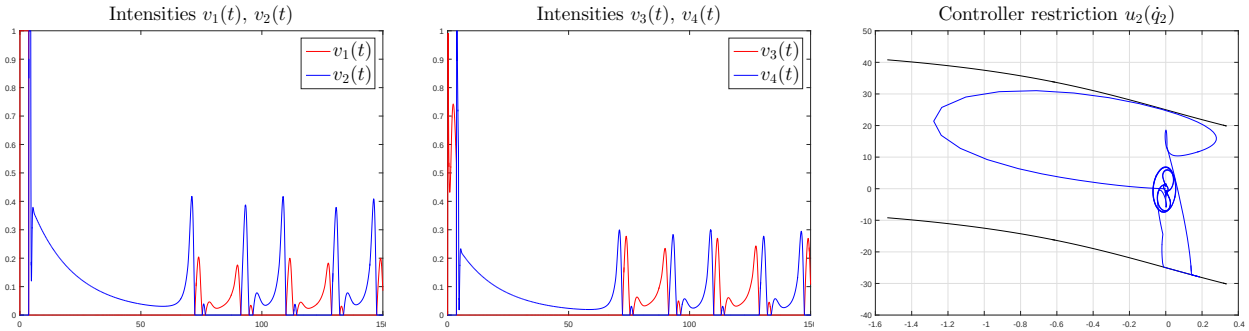

Figure 14: Intensities of the muscles C_{C1} and C_{C2} (left), intensities of the muscles C_{C3} and C_{C4} (middle), feasible range of u_2 (right).

The determination of the gain factor depends primary on the error of q_1, because q_2 stays inside the λ-area. But, due to the adaptation law, the gain parameter decreases and the angles leave the λ-area, which results in a little bit periodic behavior. To reduce the behavior of the angles at $t > 70s$, the range of the λ-tolerance area is reduced.

Simulation 7 - advanced λ-stabilizer with new adaptation, saturation and new accuracy:
In this simulation, we use the maximum-norm as well as in Simulation 6. Moreover, we diminish the λ-tolerance to $\lambda_i = 0.02$. The Figures 15 and 16 shows the results.

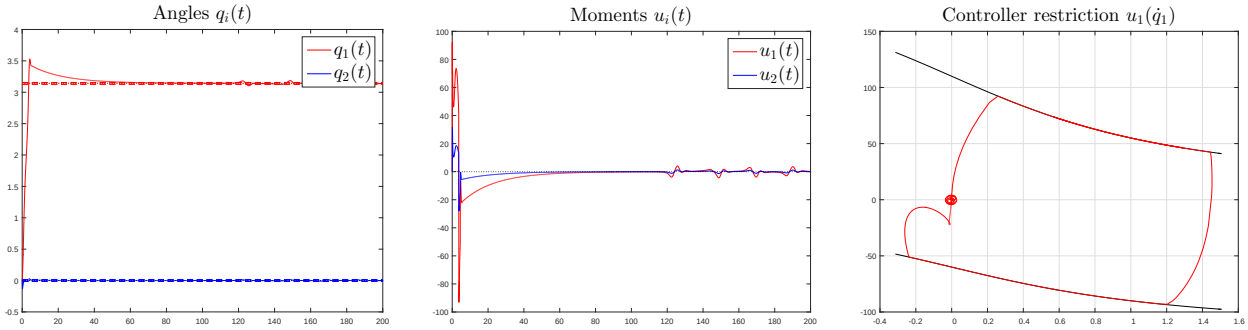

Figure 15: Joints angles q_i (left), control inputs u_i (middle), feasible range of u_1 (right).

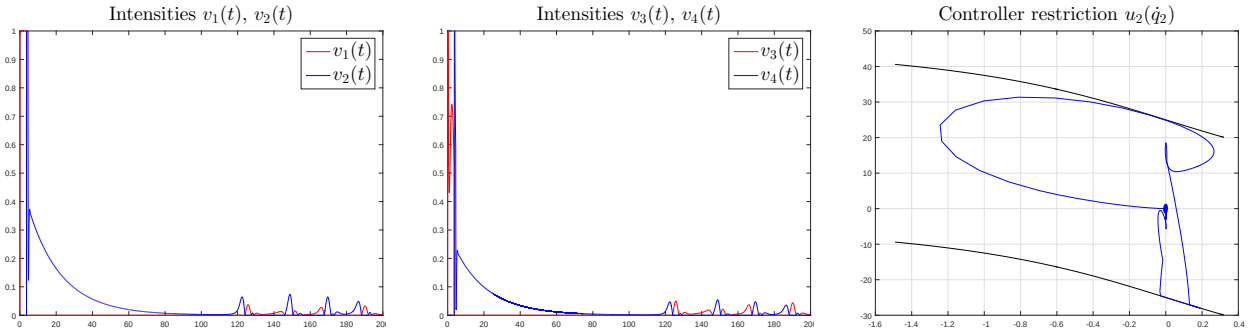

Figure 16: Intensities of the muscles C_{C1} and C_{C2} (left), intensities of the muscles C_{C3} and C_{C4} (middle), feasible range of u_2 (right).

After reaching the very small λ-tolerance area, the angles are hold therein more stable. After about $t = 120\,s$ the gain factor gets so low, that the output angles leave the tolerated area and the process of re-stabilization starts. But, one can clearly see a much better system behavior.

Summarizing, the mentioned unlike, periodic behavior of the output angles after leaving the λ-area is due to the design of the adaptation law. We allow the gain factor to, analytically, converge to zero. This has to be eliminated to keep the output inside the area, in, for example, setting a fixed lower bound. But, this will conversely influence the system and controller behavior if we deal with changing environmental conditions to which the controller has to adjust its behavior again. But overall, we achieve good stabilizing results.

Conclusions

In this work, various controllers were presented, to control a biologically inspired manipulation system actuated by muscle-like actuators. Thereby, saturated adaptive stabilizing strategies have been developed and tested. Different possibilities of these controllers were demonstrated how to implement the control variables by using an intensity controlling. The effectiveness of the control strategies were illustrated by simulations, which could serve for dimensioning of the muscle actuators, thereby the system was controlled with different muscle performance limits.
As far as possible the controller were load with similar control parameters, to compare the results. A variation of an advanced adaptive λ-stabilization shows the best results in velocity and accuracy of the stabilization. The main aspect of the advanced part of the λ-stabilization makes sure, that the gain factor can decrease inside the λ-tolerance area. By adding an error vector assuming with maximum norm, the behavior of the angles can be improved.

References

[1] Awrejcewicz J., Reshmin S.A., Wasilewski G., Kudra G.(2008) Swing up a double pendulum by simple feedback control. Proceedings ENOC 2008, St. Petersburg, Russia.

[2] Behn C. (2005) Contributions to the adaptive control of bio-inspired systems. Cuvillier, Göttingen, Germany.

[3] Behn C., Loepelmann P., Steigenberger J. (2015) Analysis and simulation of adaptive control strategies for uncertain bio-inspired sensor systems. *Mathematics In Engineering, Science and Aerospace (MESA)* 6(3), pp. 567–588.

[4] Gluck T., Eder A., Kugi A. (2013) Swing-up control of a triple pendulum on a cart with experimental validation. *Automatica* 49(3), pp. 801–808.

[5] Ilchmann A. (1993) Non-Identifier-Based High-Gain Adaptive Control. Lecture Notes in Control and Information Sciences 189, Springer, London.

[6] Abeßer H., Behn C., Steigenberger J., Zimmermann K. (2002) Steueraufgaben für Zweiarm-Roboter mit muskelähnlichen Antrieben. Proc. 47. International Scientific Colloquium, Ilmenau, Germany.

[7] Ortega R., Loría A., Nicklasson P.J., Sira-Ramírez H. (1998) Passivity-based Control of Euler-Lagrange Systems. Springer, London.

[8] Siedler K., Behn C. (2016) Adaptively Controlled Dynamical Behavior of Sensory Systems based on Mechanoreceptors. *International Journal of Structural Stability and Dynamics* in press

[9] Schmalz T. (1994) Biomechanical Modeling of Human Motion. Schorndorf, Germany.